JACS
JOURNAL OF THE AMERICAN CHEMICAL SOCIETY

Article

pubs.acs.org/JACS

Size-Dependent Partitioning of Nano/Microparticles Mediated by Membrane Lateral Heterogeneity

Tsutomu Hamada, Masamune Morita, Makiyo Miyakawa, Ryoko Sugimoto, Ai Hatanaka, Mun'delanji C. Vestergaard, and Masahiro Takagi*

School of Materials Science, Japan Advanced Institute of Science and Technology, 1-1 Asahidai, Nomi, Ishikawa 923-1292, Japan

Supporting Information

ABSTRACT: It is important that we understand the physical, chemical, and biological mechanisms that govern the interaction between nanoparticles (NPs) and heterogeneous cellular surfaces because of the possible cytotoxicity of engineered nanomaterials. In this study, we investigated the lateral localization of nano/microparticles within a biomimetic heterogeneous membrane interface using cell-sized two-phase liposomes. We found that lateral heterogeneity in the membrane mediates the partitioning of nano/microparticles in a size-dependent manner: small particles with a diameter of ≤200 nm were localized in an ordered phase, whereas large particles preferred a fluidic disordered phase. This partitioning behavior was verified by temperature-controlled membrane miscibility transition and laser-trapping of associated particles. In terms of the membrane elastic energy, we present a physical model that explains this localization preference of nano/microparticles. The calculated threshold diameter of particles that separates the particle-partitioning phase was 260 nm, which is in close agreement with our observation (200 nm). These findings may lead to a better understanding of the basic mechanisms that underlie the association of nanomaterials within a cell surface.

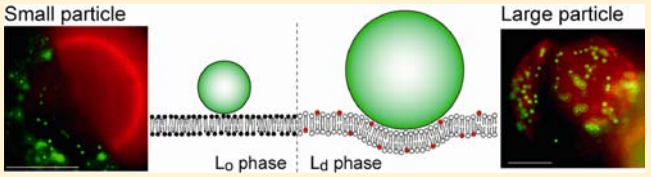

INTRODUCTION

Over the past decade, nanoscience and nanotechnology have been the focus of increasing interest to achieve advances in functional nanomaterials, such as carbon nanotubes, dendrimers, and gold nanoparticles,[1−3] since materials at a nanoscale exhibit properties that are different from those of bulk materials. By taking advantage of such unique characteristics, researchers have developed methods for the application of nanoparticles (NPs) to biological systems, such as quantum dot tags, drug-delivery systems, and MRI contrast agents.[4,5] However, the cytotoxic effects of NPs are not well understood and need to be elucidated to ensure safe handling and engineering.[6−8] NPs have been shown to adhere to and/or be internalized on the plasma membrane surface before being transported into the cytosol or nucleus.[9] It is important that we understand the physical, chemical, and biological mechanisms that govern the interaction between NPs and the cell surface, which is a soft interface ∼5 nm thick with a lipid bilayer.[10−12] Basically, the physicochemical interaction of NPs with an interface is expected to be described by the Derjaguin and Landau, Verwey and Overbeek (DLVO) theory, which includes van der Waals and electrostatic forces.[13] Along these lines, there have been many studies on the engineering of surface properties of NPs.[14,15] However, the effects of the elastic feature of the lipid membrane itself as a self-assembled soft material are not well understood. The intrinsic mechanical properties of membranes may affect the interaction between particles and the soft interface.[16]

Plasma membranes are not just a surface in which proteins are embedded, but rather they dynamically organize their interfacial structures.[17] Within membranes, microdomains called lipid rafts are formed to effectively produce lateral compartments with high lipid order and slow dynamics.[18] Bilayer lateral heterogeneity is considered to be a form of order−disorder phase separation that develops due to the interaction between membrane lipids.[19] The organized domains are expected to play an important role in the selective associations of materials during molecular-binding events, such as signaling or toxic processes.[20,21] This indicates that the mechanical properties of membranes, such as lateral fluidic heterogeneity, are coupled to functional molecular recognition within the membrane surface.

To clarify the physicochemical properties of heterogeneous membranes, several studies have considered model membrane systems using cell-sized multicomponent liposomes that phase-separate into domains.[22,23] Liposomes that are simply composed of saturated and unsaturated lipids together with cholesterol produce lateral domains within bilayer membranes. The equilibrium phase diagram of ternary lipid systems has been well characterized,[23] and the membrane phase can mainly be classified into three states: liquid-disorder (Ld), liquid-order (Lo), and solid-order (So).[24] Microscopic domain structures due to order−disorder phase separation have been observed in cell-sized liposomes with specific mixing compositions.[25] The two-liquid coexistence between Lo and Ld phases has received much attention because the Lo phase is expected to correspond to lipid rafts of the physiological membrane.[25−27] Notably,

Received: February 8, 2012
Published: August 8, 2012

 © 2012 American Chemical Society dx.doi.org/10.1021/ja301264v | J. Am. Chem. Soc. 2012, 134, 13990−13996

solid−liquid coexistence between the So and Ld phases is often produced in model membranes under altered membrane conditions, such as a decrease in the cholesterol fraction[28] or under the application of membrane tension.[29] Studies with these simple model membrane systems are invaluable for elucidating how molecules and materials interact with heterogeneous membranes, since they are controllable and specific interactions can be easily understood.[30] Recently, such membrane systems have been used to study Lo-/Ld-phase partitioning for several signaling proteins and their membrane anchors.[31] Previously, we revealed that a cytotoxic peptide, Alzheimer's amyloid β, was selectively localized in the lateral compartments of phase-separated Lo/Ld and So/Ld membranes in a peptide aggregation-dependent manner.[32,33]

In this study, we investigated the association of polystyrene nano/microparticles within biomimetic membrane interfaces with lateral heterogeneity, such as two-phase liposomes. At a heterogeneous membrane surface with Lo/Ld phase separation, nano/microparticles were selectively distributed in a size-dependent manner: large particles localized in the Ld phase, while small particles localized in the Lo phase. In contrast, all of the nano/microparticles showed partitioning into the So phase in So/Ld separated membranes. We discuss the mechanism that underlies the selective association of nano/microparticles by considering the intrinsic mechanical properties of fluid membranes.

MATERIALS AND METHODS

Materials. Dioleoyl L-α phosphatidylcholine (DOPC), dipalmitoyl L-α phosphatidylcholine (DPPC), and cholesterol (Chol) were obtained from Avanti Polar Lipids (Alabaster, AL). The fluorescent phospholipid, *N*-(rhodamine red-X)-1,2-dihexadecanoyl-*sn*-glycero-3-phosphoethanolamine triethylammonium salt (rho-PE, λ_{ex} = 560 nm, λ_{em} = 580 nm) was obtained from Invitrogen (Carlsbad, CA). Fluoresbrite yellow green polybead microspheres (YG polybeads, λ_{ex} = 441 nm, λ_{em} = 585 nm) with diameter of 50, 100, 200, and 500 nm, Fluoresbrite multifluorescent microspheres (multifluorescent polybeads, λ_{ex} = 377, 517, and 588 nm, λ_{em} = 479, 546, and 612 nm) with a diameter of 1000 nm, and Polybead Microspheres with a diameter of 1000 nm were obtained from Polysciences (Warrington, PA). There was no apparent difference in the phase-partitioning behavior between these two different 1000-nm particles with or without fluorescence. Deionized water was obtained using a Millipore Milli Q purification system.

Preparation of Nano/Microparticles. Before using nano/microparticles, we removed surfactants in the stored solution. The original solution was diluted 5-fold by deionized water. The solution was centrifuged (14500 rpm, several min), and the top clear layer was replaced with deionized water. This step was repeated 3−5 times. To eliminate aggregations, the 50-nm and 100-nm particle solutions were passed through a 200-nm porous filter (Steradisc 25, Kurabo, Osaka, Japan), and the 200-nm particle solution was passed through a 500-nm porous filter. We then prepared 10-fold diluted nano/microparticles solutions with 0.1 M sucrose for liposome hydration. We measured the ζ potential of NPs using a Zetasizer Nano ZS (Malvern Instruments, Worcestershire, United Kingdom) at 25 °C.

Preparation of Cell-Sized Liposomes with Lateral Heterogeneity. Cell-sized liposomes were prepared using an electroformation method.[34] A solution of the desired lipids (10 mg/mL in chloroform) was deposited on the conducting face of an ITO-coated slide glass (8−12 Ω/sq, Sigma-Aldrich, MO). After the glass was heated at 60 °C for ∼5 min, a single drop of chloroform was added to spread the lipid mixture to obtain a thin lipid film. The lipid film was dried overnight in a vacuum. The sample glass was covered with another ITO glass using a silicon rubber spacing of ∼1 mm. The chamber was then filled with ∼300 μL of 0.1 M sucrose containing nano/microparticles. An alternating current voltage of 1.0 V and 10 Hz was applied with a function generator (FG-281, TEXIO, Japan) for 3 h at 50 °C. The vesicle solution was carefully extracted from the chamber using a plastic syringe. The final concentration was 1−2 mM lipids (DOPC/DPPC/Chol) and 0.5 mol % rho-PE. The liposomes were composed of DOPC/DPPC = 1:1 with (25−30 mol %) or without Chol to produce Lo/Ld or So/Ld phase separation, respectively.

Microscopic Observation. The association of NPs on the liposome surface was observed using optical (phase-contrast and fluorescence) microscopy (IX71, Olympus, Japan). Standard filter sets (U-MWIG3: ex 530−550 nm, dichroic mirror 570 nm, em 575 nm, and U-NIBA3: ex 470−495 nm, dichroic mirror 505 nm, em 510−550 nm) were used to monitor the fluorescence of rho-PE and YG polybeads, respectively. The temperature of the samples was carefully controlled within ±0.1 °C using a microscope stage (type 10021, Japan Hitec). The infrared laser used for optical trapping was an ytterbium fiber laser (model YLM-2-1064-LP, IPG laser) at a wavelength of 1064 nm (0.10 W). The laser beam was reflected by a dichroic mirror and focused through an objective lens (UPlanSApo, 100×, NA = 1.40). We used a laser-trapping system to transport a membrane-associating particle. First, we confirmed that the laser did not induce changes in the morphology or phase structure of the vesicles.

RESULTS

We prepared cell-sized liposomes with aqueous solutions containing nano/microparticles by electroformation.[34] It has previously been reported that polystyrene particles spontaneously adhere to a phosphatidylcholine (PC) membrane surface.[35−37] Here, we used saturated and unsaturated PC lipids (dipalmitoyl L-α phosphatidylcholine, DPPC, and dioleoyl L-α phosphatidylcholine, DOPC) together with cholesterol (Chol) to form two-phase membranes with lateral heterogeneity. First, we used a ternary mixture of DOPC/DPPC/Chol = 37:37:26 (molar ratio) to produce two-liquid Lo/Ld phase separation. The membrane contained 0.5 mol % of a red-fluorescent lipid, rho-PE, which preferentially partitions into the Ld phase.[32] Additionally, to monitor the location of nano/microparticles, we used green-fluorescent particles, YG polybeads. The measured ζ potentials of nano/microparticles with different diameters were essentially equal: −33.9 ± 1.2, −39.4 ± 0.4, −35.7 ± 0.2, and −38.3 ± 1.0 mV for 50-, 100-, 200-, 500-nm YG polybeads. Figure 1 shows typical fluorescent images of liposome surfaces that were simultaneously stained with rho-PE and YG polybeads. We found that nano/microparticles localized in a particular membrane phase depending on their sizes. Small particles with a diameter of 50 or 100 nm tended to localize in the Lo phase (Figure 1a and also see Figure S1a in the Supporting Information [SI]), whereas large 500- and 1000-nm particles were partitioned into the Ld phase (Figure 1b and also see Figure S1c in the SI). The localization of intermediate 200-nm particles appeared to be random (Figure S1b in the SI); 200-nm particles in some liposomes were partitioned into the Lo phase, and those in others were partitioned into the Ld phase. Notably, the absence of the selective partitioning was also observed, which was not often observed with other particle sizes. In our experiments, we did not observe the unbinding event of these membrane-associated particles. Notably, although most of the adhering particles showed random thermal motions on membrane surfaces, microscopic snapshots indicate the possibility of particle aggregation (Figure 1b and Figure S1c [SI]). The linear particle aggregation within fluid membranes has been recently reported in simulations.[38] Further experimental developments on the quantitative analysis of the motions, such as diffusion,

dx.doi.org/10.1021/ja301264v | J. Am. Chem. Soc. 2012, 134, 13990−13996

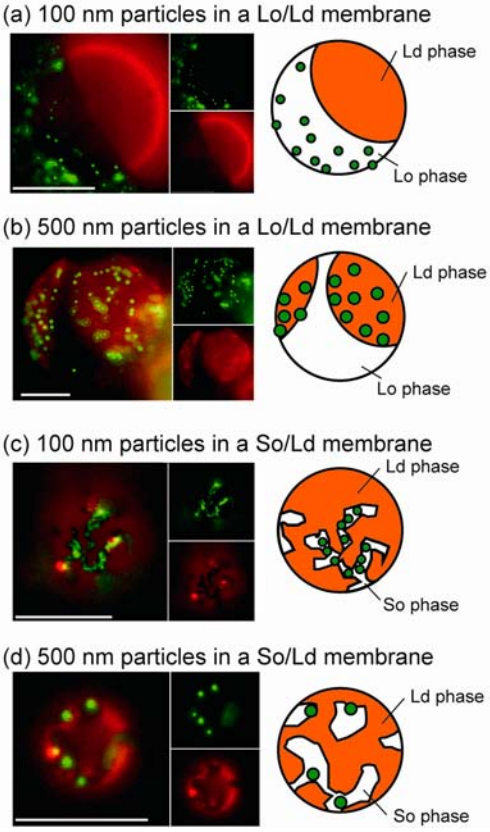

Figure 1. Selective localization of nano/microparticles (green) on phase-separated membranes, where the membranes were stained with rho-PE (red), which partitions into the Ld phase. (a) Particles 100 nm in diameter were distributed in the Lo phase of an Lo/Ld membrane; (b) 500-nm particles were localized in the Ld phase of an Lo/Ld membrane; (c) 100-nm particles were partitioned into the So phase of an So/Ld membrane; and (d) 500-nm particles were localized in the So phase of an So/Ld membrane. Scale bars are 10 μm.

aggregation, and location, of partitioning particles are underway.

To better understand the effects of membrane phase properties on nano/microparticle partitioning, we prepared liposomes of DOPC/DPPC = 50:50 (molar ratio) without Chol. This binary system does not exhibit two-liquid Lo/Ld phase organization and instead shows solid–liquid So/Ld separation, since the Lo phase is a unique structure that is only seen with membranes that contain sterol.[24] There is a clear difference in phase boundary structures between two-liquid and solid–liquid separation: while liquid domains show circular shapes due to line tension (Figure 1a,b), solid domains have a random boundary structure (Figure 1c,d). As shown in Figure 1c,d (also see Figure S2 in the SI), within So/Ld membranes, nano/microparticles with diameters of 50, 100, 200, 500, and 1000 nm were all localized in the So phase. In contrast to the Lo/Ld membranes shown in Figure 1a,b, the lateral distribution of particles in So/Ld membranes does not depend on the particle size. Our results correspond to the equilibrium configuration, because we started the observation after 3-h incubation time for the particle–membrane mixing procedure.

Next, we investigated whether the selective localization of particles is reproduced during the miscibility (mixing/demixing) transition. At low temperature, the membranes are phase-separated. An increase in temperature above the miscibility transition temperature alters the membrane such that the two-phase membrane becomes a one-phase membrane.[28] Figure 2 shows the membrane surface structure of a

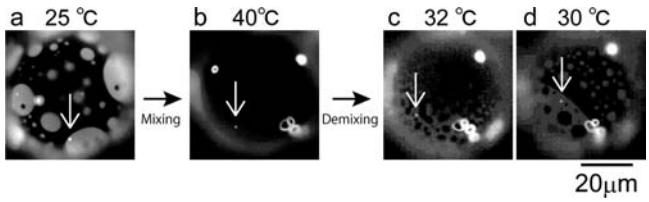

Figure 2. Reproducibility of the selective association of a particle during the mixing/demixing transition. In the images, the arrows indicate a 1000 nm particle that localizes in the Ld phase.

single Lo/Ld liposome with 1000-nm particles under a change in temperature. In this particular analysis, to monitor the behaviors of both particles and membranes in real-time, we used particles with the same red fluorescence, multifluorescent polybeads, as the membrane tag (rho-PE). Before the temperature change, 1000-nm particles were localized in the Ld phase region (Figure 2a). We then increased the temperature from 25 to 40 °C at 10 °C/min. When the temperature increased over the miscibility transition temperature (~30 °C),[28] the membrane became homogeneous without domains. The particles exhibited random thermal motion in the uniform membrane surface (Figure 2b). When we decreased the temperature (at −10 °C/min) to induce Lo/Ld phase separation,[39] the particles again associated in the Ld phase region during domain growth (Figure 2c,d).

We, then, obtained quantitative data showing the selective partitioning for each particle (Figure 3). First, we incubated the

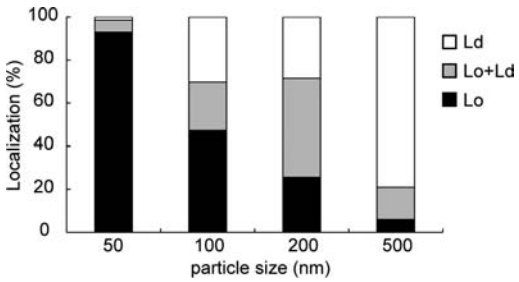

Figure 3. Selective partitioning of nano/microparticles within Lo/Ld membranes. N = 71 (50-nm particles), 178 (100-nm particles), 168 (200-nm particles) and 67 (500-nm particles).

sample at 60 °C for over an hour after the vesicle preparation with electroformation. Then, we put the sample at 25 °C for 3 days to achieve equilibrium configuration, and counted the localization preference of particles. Liposomes with 50- and 100-nm particles mostly showed Lo-phase partitioning (93% and 47%, respectively). In contrast, the absence of selective localization (adsorption on both phases) was predominantly observed in liposomes with 200-nm particles (46%). Liposomes with 500-nm particles largely exhibited Ld phase localization (79%).

To better understand the characteristics of the particles associated within phase-separated domains, we manipulated particles with lasers. With the use of laser-trapping as an experimental tool, a particle can be fixed at the focus of an IR laser.[40] We trapped a 1000-nm particle (multifluorescent polybead), which was localized in the Ld phase of an Lo/Ld

dx.doi.org/10.1021/ja301264v | J. Am. Chem. Soc. 2012, 134, 13990–13996

liposome. We then transported the particle laterally on the surface of the liposome (Figure 4; the shift of the laser focus is

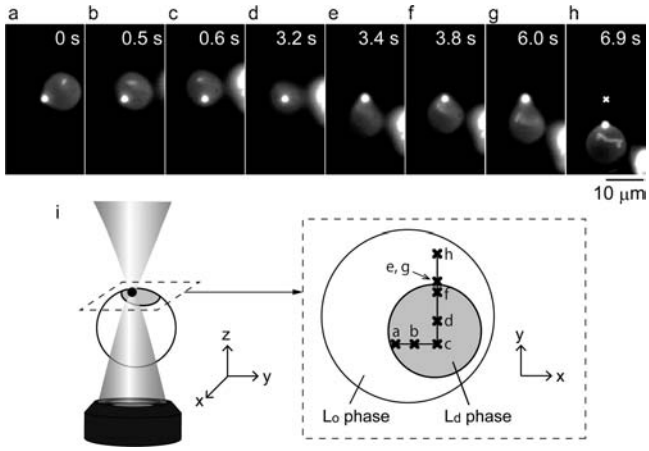

Figure 4. Movement of an associated particle using laser tweezers. (a–h) Fluorescent image sequences of a laser-trapped 1000-nm particle within an Ld domain. The laser trap is positioned at the center of the images. (i) The shift of the trapping point corresponding to each image (a–h) is shown schematically.

shown in Figure 4i). Although the trapped particle was transported following the shift in position of the laser focus within the Ld phase (Figure 4a–e), the particle could not exit the Ld region across the phase boundary (Figure 4e–h). When we shifted the focus position from the Ld to the Lo phase region, the shape of the Ld domain was slightly deformed to retain the associated particle (Figure 4e). After particle movement was stopped, the domain reverted to its original spherical shape due to line tension of the phase boundary (Figure 4f). Further shifting of the focus toward the Lo region resulted in the departure of the particle from the focus position. However, the particle still remained in the original Ld phase domain (Figure 4g,h).

Furthermore, we explored this particle–membrane interaction to move lateral membrane domains by laser-trapping an associated particle. It is important that we are able to control such mesoscopic organized structures of soft-matter complexes so that we can better understand the physical mechanism of self-organization and develop soft nanotechnology for specific functions. Figure 5 shows a clear demonstration of the optical transportation of an Ld-phase domain on a membrane surface. When we trapped a 1000-nm particle in an Ld domain and gradually shifted the position of the focus, the position of the Ld domain moved in association with the trapped particle to achieve domain fusion. These findings are an example of an engineered soft-matter system: the formation of lateral domains mediates nano/microparticles partitioning (Figure 2), and membrane-associated nano/microparticles enable the optical manipulation of lateral domains (Figure 5).

■ DISCUSSION

The present results reveal that lateral heterogeneity of the membrane mediates the phase-partitioning of nano/microparticles in a size-dependent manner. Within phase-separated two-liquid (Lo/Ld) membranes, smaller particles of ≤200 nm were localized in the Lo region (Figure 1a), while larger particles of ≥200 nm were partitioned into the Ld region (Figure 1b). When we excluded Chol to achieve solid–liquid

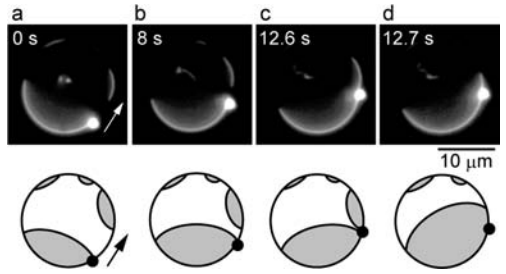

Figure 5. Controllable fusion of Ld phase domains by the optical transfer of an associated particle. White arrow indicates the direction of the applied force. We trapped a 1000-nm particle in an Ld domain, and gradually shifted the position of the focus toward another Ld domain (a). The Ld domain moved together with the trapped particle (b), so that it eventually collided with the other domain (c) and fused (d). Rapid movement of the focus position led to detachment of the trapped particle, as shown in Figure 3h.

(So/Ld) phase separation, all of the nano/microparticles, regardless of size, were localized in the So phase (Figure 1c,d). The partitioning of nano/microparticles was reproduced during the mixing/demixing miscibility transition (Figure 2), indicating that this behavior of nano/microparticles is mediated by the thermodynamic characteristics of the lipid membranes. Recently, a few theoretical investigations have reported on the interaction of particles with multicomponent membranes.[41,42] This is the first experimental report on the interaction between particles and heterogeneous membrane systems, although there have been several studies on membrane–colloid interactions with homogeneous cell-sized liposomes.[35−37,43−48]

This selective association may be attributed to the mechanical properties of the heterogeneous membranes, since the surface properties of polystyrene particles, such as the ζ potential, do not change with their size. It has been known that polystyrene microparticles spontaneously adhere to PC membranes.[35−37] We also confirmed that small (100 nm) and large (500 nm) particles can adhere to both Ld-only (DOPC) and Lo-only (DPPC/Chol = 50:50) membranes (see the SI). The adhesion trend in the one-phase liposomes was essentially the same as that observed in the two-phase liposomes: 100-nm particles tend to adhere on Lo-only liposomes, and 500-nm particles relatively adhere on Ld-only liposomes (Figure S3, SI). We here discuss the mechanism of the partitioning of adhered nano/microparticles within two-phase membrane interfaces from a phenomenological perspective. We assume that particles simply contact a fluid interface without disrupting the membrane bilayer.[49] When a particle strongly adheres to a membrane surface, the membrane curves around the particle's periphery.[50−52] The threshold particle radius r^* for membrane deformation to wrap a particle is estimated to be $r^* \approx (2\kappa/w)^{1/2}$,[49] where w is the adhesion energy (J·m^{-2}), κ is the bending stiffness of the membrane (J), and the spontaneous curvature of the membrane is zero. This indicates that the adhesion of larger particles of $r > r^*$ tends to induce the deformation of membrane curvature, while smaller particles of $r < r^*$ do not alter such mesoscopic membrane structures. When a membrane exhibits bending deformation due to the association of large particles, the free energy cost per unit area is shown as

$$\Delta F = \frac{\kappa}{2}(c_1 + c_2 - c_0)^2 \quad (1)$$

dx.doi.org/10.1021/ja301264v | J. Am. Chem. Soc. 2012, 134, 13990−13996

where c_1 and c_2 are the two principal curvatures, and c_0 is the spontaneous curvature.[53] Since the free energy is proportional to κ, a difference in bending stiffness between the Ld and Lo phases ($\kappa_{Ld} < \kappa_{Lo}$) leads to $\Delta F_{Ld} < \Delta F_{Lo}$, indicating that large particles of $r > r^*$ tend to distribute in the Ld phase of Lo/Ld membranes. In contrast, for small particles of $r < r^*$, the effect of bending deformation is insignificant. However, when particles are situated close to the membrane surface, thermal undulation of the membrane should be restricted in a finite space. For the adhesion of small particles of $r < r^*$, the change in membrane undulation may be considered instead of bending deformation. The free energy cost per unit area for restricted undulation is expressed as

$$\Delta F = \frac{3(k_B T)^2}{2\pi^2 \kappa} \frac{1}{d^2} \quad (2)$$

where d is the length of the space.[54] The free energy is inversely proportional to κ, indicating that $\Delta F_{Ld} > \Delta F_{Lo}$, which explains why smaller particles tend to localize in the Lo phase while larger particles partition into the Ld phase, in agreement with our experimental results. Notably, for the interaction of large particles, the contribution of undulation energy is expected to be much smaller than that of bending energy (see the SI). It should be also mentioned that here we observed quasi-spherical liposomes, and the membrane area and internal volume are essentially constant during the experiments. The change in membrane area or internal volume would influence the phase-partitioning behavior of particles, because additional parameters, such as bilayer stretching and/or membrane excess area, should be considered.

For simplicity, we assume that the adhesion energy is essentially derived from van der Waals interaction between the surfaces of a polystyrene and lipid, since electrostatic interactions may be ignored between the negatively charged particles and neutral phospholipid (PC) membranes. The adhesion energy can be expressed as $w = A/12\pi D^2$, where A is the Hamaker constant of $A = ((A_{polystyrene})^{1/2} - (A_{water})^{1/2})((A_{lipid})^{1/2} - (A_{water})^{1/2})$, and D is the distance between the surfaces of the particle and membrane.[13] By substituting $\kappa = 1.2 \times 10^{-19}$ J,[55] $A_{polystyrene} = 6.5 \times 10^{-20}$ J, $A_{lipid} = 8.0 \times 10^{-20}$ J, $A_{water} = 3.7 \times 10^{-20}$ J, and $D = 3$ nm,[13] we obtain $r^* = 130$ nm (260 nm diameter), which is in close agreement with our observation (200 nm). This also explains the absence of the selective partitioning in some liposomes with particles of 200 nm. For So/Ld membranes, the surface of the So phase does not show fluidic properties such as curvature deformation and thermal undulation. The partitioning of small particles into the So phase is energetically preferable for the same reason as the Lo-phase partitioning in Lo/Ld membranes. However, the mechanism for the So-phase partitioning of large particles is still unclear. Since So membranes are essentially nondeformable, the gain of adhesion energy is expected to be less. We should consider some factors for an increase in adhesion energy on So-phase membranes. The absence of thermal undulation in the So phase decreases the distance between the particle and membrane, leading to an increase in adhesion energy. In addition, the roughness of the So-membrane surface may somewhat fit a colloidal surface to gain a large contact area. It should also be mentioned that the surface properties of So phase, such as Hamaker constant and/or charge characteristics, are possibly different from the liquid phases. Our results indicate that contacting materials tend to localize into the So region within phase-separated membranes. We also reported that amyloid β peptides tend to localize into the So phase of So/Ld membranes.[33] An So phase has been reported to be produced in model membrane systems under a decrease in the Chol fraction[28] and an increase in membrane tension.[29] Within actual plasma membranes, a change in the fluidity of membrane domains may be a key step for cytotoxic processes, since all materials tend to aggregate in the So-phase membrane. The critical particle size depends on the particle−lipid interaction and membrane stiffness. It is predictable that an increase in attractive forces, such as the introduction of electrostatic attraction or particles with a large Hamaker constant, decreases the critical size. The increase in membrane stiffness, such as highly mixing fractions of DPPC, tends to increase in the critical size. It should be noted that carboxyl-modified polystyrene nanoparticles with a high negative charge can adsorb on PC large unilamellar vesicles and change its phase properties.[56] It was also reported that, in the supported PC bilayer systems, polystyrene nanoparticles disrupt the bilayer to form holes, probably due to hydrophobic interaction.[57]

We only studied nano/microparticles with a spherical structure. Nanomaterials with different shapes, such as carbon nanotubes (nonbiological) as well as protein/peptide, DNA, and virus (biological), may exhibit different partitioning behaviors. Parameters such as the degree of asymmetry of the specific shape should be important. It is also crucial to consider other membrane interactions, such as bilayer insertion, in addition to simple adhesion (which we described above) to fully unravel the binding events of materials on heterogeneous bilayer membranes.[33] We did not consider the insertion of particles into the lipid bilayer, because the diameter ($\geq$50 nm) of particles used in this study is 10 times greater than the thickness of the lipid bilayer ($\sim$5 nm). Much smaller nanoparticles may exhibit bilayer insertion, leading to the disruption of the membrane.[42,58] Further experimental developments to clarify the phase-partitioning of nanoparticles with a diameter of $\leq$50 nm are underway.

The results of our laser-manipulation experiments also support the partitioning of nano/microparticles within a lateral membrane compartment. A trapped 1000-nm particle was transported after the laser focus was shifted inside the Ld phase of the Lo/Ld membrane but could not migrate from the Ld region across a phase boundary (Figure 4). This indicates that the partitioning energy is greater than the energy of the laser-mediated particle-transportation that we applied here. If we consider the bending energy from the curved region that is needed to wrap the particle, the energy that governs partitioning of the particle would be expected to be greater than the estimated transportation energy (see the SI).

■ CONCLUSIONS

In summary, we have demonstrated the selective partitioning of polystyrene nano/microparticles (50-, 100-, 200-, 500-, and 1000-nm diameters) within a biomimetic heterogeneous membrane interface using phase-separated cell-sized liposomes. We found that the size of the particles determined the partitioning phase without a change in the surface property of the particles. This association preference can be explained by considering the membrane elastic energy with the fluidic difference between two coexisting phases; small particles tend to be localized in the ordered phase, while large particles prefer the disordered phase. The calculated threshold diameter of nano/microparticles that separates the particle-partitioning

phase was 260 nm, which is in close agreement with our observation (200 nm). These findings strongly indicate that not only specific molecular interactions, such as those of receptor proteins, but also the mechanical properties of the fluid bilayer itself play an important role in the selection of associating materials into lateral compartments. Cells may take advantage of the membrane thermodynamic characteristics to recognize contacting materials. Desai et al., observed the size-dependent uptake of particles in a cell.[59] In further studies, it may be useful to investigate the dynamical behavior of nanoparticle–membrane systems, such as endocytosis, since nanomaterials that are in contact with plasma membranes are eventually engulfed by wrapping.[9] Theoretical investigations have also been developed.[60,61] Biological raft domains are expected to function as platforms that form such endocytic carriers,[21] and endocytosis-like transformation has been demonstrated using a cell-sized model system.[62]

■ ASSOCIATED CONTENT

Supporting Information

Other images of the selective partitioning of micro/nanoparticles within phase-separated liposomes, adsorption of particles on homogeneous membranes, comparison between bending and undulation energies, and an energy comparison of laser-transportation and phase-partitioning. This material is available free of charge via the Internet at http://pubs.acs.org.

■ AUTHOR INFORMATION

Corresponding Author

takagi@jaist.ac.jp

Notes

The authors declare no competing financial interest.

■ ACKNOWLEDGMENTS

Technical assistance from Ms. Shino Mizuno is greatly appreciated. We thank Dr. Masatoshi Ichikawa (Kyoto University) for providing fruitful discussions. This work was supported by KAKENHI Grants-in-Aid for Scientific Research B and C and Young Scientists B from JSPS, by a Grant on Priority Areas "Soft Matter Physics" and "Soft Interfaces" from MEXT of Japan, and by a Sunbor Grant from the Suntory Institute for Bioorganic Research.

■ REFERENCES

(1) Baughman, R. H.; Zakhidov, A. A.; de Heer, W. A. *Science* **2002**, *297*, 787.
(2) Bronstein, L. M.; Shifrina, Z. B. *Chem. Rev.* **2011**, *111*, 5301.
(3) Daniel, M. C.; Astruc, D. *Chem. Rev.* **2004**, *104*, 293.
(4) Ke, P. C.; Lamm, M. H. *Phys. Chem. Chem. Phys.* **2011**, *13*, 7273.
(5) Mody, V. V.; Nounou, M. I.; Bikram, M. *Adv. Drug Delivery Rev.* **2009**, *61*, 795.
(6) Stark, W. J. *Angew. Chem., Int. Ed.* **2011**, *50*, 1242.
(7) Nel, A.; Xia, T.; Madler, L.; Li, N. *Science* **2006**, *311*, 622.
(8) Maynard, A. D.; Aitken, R. J.; Butz, T.; Colvin, V.; Donaldson, K.; Oberdörster, G.; Philbert, M. A.; Ryan, J.; Seaton, A.; Stone, V.; Tinkle, S. S.; Tran, L.; Walker, N. J.; Warheit, D. B. *Nature* **2006**, *444*, 267.
(9) Zhao, F.; Zhao, Y.; Liu, Y.; Chang, X.; Chen, C.; Zhao, Y. *Small* **2011**, *7*, 1322.
(10) Roiter, Y.; Ornatska, M.; Rammohan, A. R.; Balakrishnan, J.; Heine, D. R.; Minko, S. *Nano Lett.* **2008**, *8*, 941.
(11) Park, J.; Lu, W. *Phys. Rev. E: Stat., Nonlinear, Soft Matter Phys.* **2009**, *80*, 021607.
(12) Lin, J. Q.; Zhang, H. W.; Chen, Z.; Zheng, Y. G. *ACS Nano* **2010**, *4*, 5421.
(13) Israelachvili, J. N. *Intermolecular and Surface Forces*; Academic Press: London, 1985.
(14) Stellacci, F.; Verma, A. *Small* **2010**, *6*, 12.
(15) Arvizo, R. R.; Miranda, O. R.; Thompson, M. A.; Pabelick, C. M.; Bhattacharya, R.; Robertson, J. D.; Rotello, V. M.; Prakash, Y. S.; Mukherjee, P. *Nano Lett.* **2010**, *10*, 2543.
(16) Tanaka, H.; Isobe, M.; Yamamoto, J. *Phys. Rev. Lett.* **2002**, *89*, 168303.
(17) McMahon, H. T.; Gallop, J. L. *Nature* **2005**, *438*, 590.
(18) Brown, D. A.; London, E. *J. Biol. Chem.* **2000**, *275*, 17221.
(19) Lingwood, D.; Simons, K. *Science* **2010**, *327*, 46.
(20) Hancock, J. F. *Nat. Rev. Mol. Cell Biol.* **2006**, *7*, 456.
(21) Simons, K.; Gerl, M. J. *Nat. Rev. Mol. Cell Biol.* **2010**, *11*, 688.
(22) Bagatolli, L.; Kumar, P. B. S. *Soft Matter* **2009**, *5*, 3234.
(23) Veatch, S. L.; Keller, S. L. *Biochim. Biophys. Acta Mol. Cell Res.* **2005**, *1746*, 172.
(24) van Meer, G.; Voelker, D. R.; Feigenson, G. W. *Nat. Rev. Mol. Cell Biol.* **2008**, *9*, 112.
(25) Veatch, S. L.; Keller, S. L. *Biophys. J.* **2003**, *85*, 3074.
(26) Baumgart, T.; Hess, S. T.; Webb, W. W. *Nature* **2003**, *425*, 821.
(27) Hamada, T.; Sugimoto, R.; Nagasaki, T.; Takagi, M. *Soft Matter* **2011**, *7*, 220.
(28) Veatch, S. L.; Keller, S. L. *Phys. Rev. Lett.* **2002**, *89*, 268101.
(29) Hamada, T.; Kishimoto, Y.; Nagasaki, T.; Takagi, M. *Soft Matter* **2011**, *7*, 9061.
(30) Hamada, T.; Sugimoto, R.; Vestergaard, M. C.; Nagasaki, T.; Takagi, M. *J. Am. Chem. Soc.* **2010**, *132*, 10528.
(31) Johnson, S. A.; Stinson, B. M.; Go, M. S.; Carmona, L. M.; Reminick, J. I.; Fang, X.; Baumgart, T. *Biochim. Biophys. Acta Biomembr.* **2010**, *1798*, 1427.
(32) Hamada, T.; Morita, M.; Kishimoto, Y.; Komatsu, Y.; Vestergaard, M.; Takagi, M. *J. Phys. Chem. Lett.* **2010**, *1*, 170.
(33) Morita, M.; Hamada, T.; Tendo, Y.; Hata, T.; Vestergaard, M.; Takagi, M. *Soft Matter* **2012**, *8*, 2816.
(34) Angelova, M. I.; Dimitrov, D. S. *Faraday Discuss. Chem. Soc.* **1986**, *81*, 303.
(35) Dietrich, C.; Angelova, M.; Pouligny, B. *J. Phys. II* **1997**, *7*, 1651.
(36) Dimova, R.; Dietrich, C.; Hadjiisky, A.; Danov, K.; Pouligny, B. *Eur. Phys. J. B* **1999**, *12*, 589.
(37) Dimova, R.; Pouligny, B.; Dietrich, C. *Biophys. J.* **2000**, *79*, 340.
(38) Šarić, A.; Cacciuto, A. *Phys. Rev. Lett.* **2012**, *108*, 118101.
(39) Saeki, D.; Hamada, T.; Yoshikawa, K. *J. Phys. Soc. Jpn.* **2006**, *75*, 013602.
(40) Ashkin, A. *Phys. Rev. Lett.* **1970**, *24*, 156.
(41) Liang, Q.; Ma, Y.-Q. *J. Phys. Chem. B* **2008**, *112*, 1963.
(42) May, S.; Harries, D.; Ben-Shaul, A. *Phys. Rev. Lett.* **2002**, *89*, 268102.
(43) Aranda-Espinoza, H.; Chen, Y.; Dan, N.; Lubensky, T. C.; Nelson, P.; Ramos, L.; Weitz, D. A. *Science* **1999**, *285*, 394.
(44) Dinsmore, A. D.; Wong, D. T.; Nelson, P.; Yodh, A. G. *Phys. Rev. Lett.* **1998**, *80*, 409.
(45) Koltover, I.; Radler, J. O.; Safinya, C. R. *Phys. Rev. Lett.* **1999**, *82*, 1991.
(46) Yu, Y.; Granick, S. *J. Am. Chem. Soc.* **2009**, *131*, 14158.
(47) Zupanc, J.; Drobne, D.; Drasler, B.; Valant, J.; Iglic, A.; Kralj-Iglic, V.; Makovec, D.; Rappolt, M.; Sartori, B.; Kogej, K. *Carbon* **2012**, *50*, 1170.
(48) Zupanc, J.; Dobnikar, A.; Drobne, D.; Valant, J.; Erdogmus, D.; Bas, E. *J. Biomed. Opt.* **2011**, *16*, 026003.
(49) Lipowsky, R.; Dobereiner, H. G. *Europhys. Lett.* **1998**, *43*, 219.
(50) Fošnarič, M.; Iglič, A.; Kroll, D. M.; May, S. *J. Chem. Phys.* **2009**, *131*, 105103.
(51) Deserno, M. *Phys. Rev. E: Stat., Nonlinear, Soft Matter Phys.* **2004**, *69*, 031903.
(52) Mkrtchyan, S.; Ing, C.; Chen, J. Z. Y. *Phys. Rev. E: Stat., Nonlinear, Soft Matter Phys.* **2010**, *81*, 011904.
(53) Helfrich, W. *Z. Naturforsch.* **1973**, *28c*, 693.

(54) Helfrich, W. *Z. Naturforsch.* **1978**, *33a*, 305.
(55) Seifert, U.; Lipowsky, R. In *Structure and Dynamics of Membranes*; Lipowsky, R., Sackmann, E., Eds.; Elsevier: Amsterdam, 1995; p 403.
(56) Wang, B.; Zhang, L.; Bae, S. C.; Granick, S. *Proc. Natl. Acad. Sci. U.S.A.* **2008**, *105*, 18171.
(57) Jing, B.; Zhu, Y. *J. Am. Chem. Soc.* **2011**, *133*, 10983.
(58) Yang, K.; Ma, Y.-Q. *Nat. Nanotechnol.* **2010**, *5*, 579.
(59) Desai, M. P.; Labhasetwar, V.; Walter, E.; Levy, R. J.; Amidon, G. L. *Pharm. Res.* **1997**, *14*, 1568.
(60) Yi, X.; Shi, X.; Gao, H. *Phys. Rev. Lett.* **2011**, *107*, 098101.
(61) Gao, H.; Shi, W.; Freund, L. B. *Proc. Natl. Acad. Sci. U.S.A.* **2005**, *102*, 9469.
(62) Hamada, T.; Miura, Y.; Ishii, K.; Araki, S.; Yoshikawa, K.; Vestergaard, M.; Takagi, M. *J. Phys. Chem. B* **2007**, *111*, 10853.